JGR Biogeosciences

RESEARCH ARTICLE
10.1029/2020JG006193

Water and Light-Use Efficiency Are Enhanced Under Summer Coastal Fog in a California Agricultural System

Sara A. Baguskas[1], Andrew J. Oliphant[1], Rachel E. S. Clemesha[2], and Michael E. Loik[3]

[1]Department of Geography & Environment, San Francisco State University, San Francisco, CA, USA, [2]Scripps Institution of Oceanography, University of California-San Diego, La Jolla, CA, USA, [3]Department of Environmental Studies, University of California-Santa Cruz, Santa Cruz, CA, USA

Key Points:

- Gross primary productivity is unchanged between foggy and clear-skies because diffuse light conditions optimize whole-plant carbon uptake
- Evapotranspiration is half that on foggy compared to non-foggy days, suggesting irrigation scheduling could be modified during fog events
- Downwelling longwave radiation correlates with a satellite-derived fog index and improves detection and characterization of fog events

Supporting Information:

Supporting Information may be found in the online version of this article.

Correspondence to:

S. A. Baguskas,
baguskas@sfsu.edu

Citation:

Baguskas, S. A., Oliphant, A. J., Clemesha, R. E. S., & Loik, M. E. (2021). Water and light-use efficiency are enhanced under summer coastal fog in a California agricultural system. *Journal of Geophysical Research: Biogeosciences*, *126*, e2020JG006193. https://doi.org/10.1029/2020JG006193

Received 3 DEC 2020
Accepted 20 APR 2021

Author Contributions:

Conceptualization: Sara A. Baguskas, Andrew J. Oliphant, Michael E. Loik
Data curation: Sara A. Baguskas, Andrew J. Oliphant, Rachel E. S. Clemesha
Formal analysis: Sara A. Baguskas, Andrew J. Oliphant, Rachel E. S. Clemesha
Funding acquisition: Sara A. Baguskas, Michael E. Loik
Investigation: Sara A. Baguskas, Andrew J. Oliphant, Rachel E. S. Clemesha
Methodology: Sara A. Baguskas, Andrew J. Oliphant, Rachel E. S. Clemesha, Michael E. Loik
Project Administration: Sara A. Baguskas

Abstract

In coastal California, the peak growing season of economically important crops is concurrent with fog events, which buffer drought stress during the dry season. Coastal fog patterns are changing, so we quantified its effects on the energy, water, and carbon fluxes of a strawberry farm located in the fog-belt of the Salinas Valley, California. We used Geostationary Operational Environmental Satellite (GOES) total albedo to detect and quantify large scale patterns of coastal fog. We used eddy covariance (EC) to quantify actual evapotranspiration and gross primary productivity (GPP) at the field scale (approximately 0.5–3 hectares) from June to September 2016. We measured canopy-scale (approximately 0.6 m^2) strawberry physiology on foggy and non-foggy days within the measurement footprint of the EC tower. Downwelling longwave radiation ($L\downarrow$), observed by a surface-mounted pyrgeometer, was consistently higher on foggy compared to clear-sky days (regardless of fog-drip), indicating that emission of longwave radiation was derived almost entirely from the cloud base. $L\downarrow$ and total GOES albedo were positively and strongly correlated ($R^2 = 0.68$, $P < 0.01$). For both field- and canopy-scales, water-use and light-use efficiency increased by as much as 50% and 70%, respectively, during foggy compared to non-foggy conditions. The initial slope of the curvilinear relationship fit between GPP and photosynthetically active radiation was twice as steep during foggy ($\alpha = 0.0395$) than non-foggy ($\alpha = 0.0210$) conditions, suggesting that the scattering of light during fog events enhances photosynthetic output of whole-plants. Our results suggest that irrigation for these fields could be rescheduled during foggy periods without sacrificing plant productivity.

Plain Language Summary

Coastal fog buffers the effects of heat and water stress on coastlands. In coastal California, the growing season of the most economically important crops occurs during the foggy summer months. The influence of coastal fog on the water use and carbon gain of farms has potential to inform future farming practices that aim to adapt to climate change. We investigated the impact of coastal fog on the water, carbon, and energy fluxes on a strawberry farm in California. We observed that water loss from plants and soil was significantly reduced during fog events due to a decrease in atmospheric stress. To our surprise, we found that total carbon gain by strawberry plants was unchanged between foggy and clear-sky days, despite a decline in plant-available light during fog events. Our results support the idea that an enhancement in diffuse, that is, scattered, light optimizes light absorption of whole-plants. Our study provides evidence that would support a reduction of irrigation during fog events without compromising crop productivity.

1. Introduction

California's agriculture sector has a large ecological footprint and farmers are under pressure to implement sustainable farming practices that combat climate change while sustaining their livelihoods. Economic models that incorporate climate change impacts on California agricultural production show a net negative impact on profits over the next 50 years (Deschenes & Kolstad, 2011). Similarly, global models predict crop yields to be negatively impacted by climate change (Challinor et al., 2014). Moreover, in California, water availability will become more scarce as temperatures rise (Dettinger et al., 2015; Williams, Seager, et al., 2015). In response to historic drought conditions, the Sustainable Groundwater Management Act (SGMA) was enacted to curtail groundwater overdraft on farms in order to sustain freshwater resources that support agriculture in the future (Rohde et al., 2017). Based on climate change impacts and scenarios, farmers should be incentivized to implement practices that minimize water-use in order to sustain crop yields

Resources: Sara A. Baguskas, Andrew J. Oliphant, Michael E. Loik
Software: Sara A. Baguskas, Andrew J. Oliphant, Michael E. Loik
Supervision: Sara A. Baguskas, Andrew J. Oliphant, Michael E. Loik
Validation: Sara A. Baguskas
Visualization: Sara A. Baguskas, Andrew J. Oliphant, Rachel E. S. Clemesha
Writing – original draft: Sara A. Baguskas, Andrew J. Oliphant, Rachel E. S. Clemesha, Michael E. Loik
Writing – review & editing: Sara A. Baguskas, Andrew J. Oliphant, Rachel E. S. Clemesha, Michael E. Loik

in the future (Jackson et al., 2011). Determining how local environmental factors control carbon and water exchange between the surface and atmosphere in agricultural systems is necessary for developing adaptive management strategies for mitigating climate change impacts on farms.

California leads in cash crop receipts in the United States (CDFA Agriculture Statistics Review, 2019). Strawberries are one of the top 10 most economically important crops in California, and the majority are grown in central coastal California (CDFA Agriculture Statistics Review, 2019). In crop year 2016–2017, strawberry production in California contributed $1.8 billion USD to the state's $46 billion USD agricultural industry and was ranked as the sixth most valuable export crop (CDFA Agriculture Statistics Review, 2016). Strawberry cultivation accounts for nearly 150 km^2 of California's coastal agricultural land (Fissell, 2018). The majority of strawberry farms are located along the central coast from Santa Cruz to Ventura County (Geisseler & Horwath, 2016). The strawberry growing season (May–October) overlaps with the occurrence of summertime coastal California fog events (Dawson, 1998; Clemesha et al., 2016). Coastal fog is commonly defined as a low-lying stratocumulus cloud that touches the ground (Torregrosa et al., 2016). Coastal fog events have also been defined to include low-lying stratocumulus clouds that may not touch the ground, but are below a specific altitude (Williams, Schwartz, et al., 2015). In this study, we use this second approach and define "coastal fog" to include low-lying (<1,000 m) stratocumulus clouds that may or may not touch the ground.

The intersection of coastal fog and agriculture depends on the inland extent of coastal fog, which is largely controlled by the coastal-inland temperature gradient, prevailing wind direction, and coastal topography (Torregrosa et al., 2016). The majority of coastal strawberry farms located in the Monterey Bay, a hotspot for strawberry production and where our study was conducted, are on the leeward side of coastal mountains and tend to be located within 4 km of the coastline. These areas are in the "fog belt," meaning that they have the highest probability of being influenced by coastal fog events when they occur (Torregrosa et al., 2016).

Spatial and temporal variability in coastal fog during the growing season can affect crop water use and carbon gain. Baguskas et al. (2018) demonstrated that strawberry plant water-use efficiency, that is, water loss per unit carbon gain, increases during fog events at the plant canopy scale (0.6 m^2). These results suggest that utilizing knowledge about conditions associated with local meteorology has the potential to increase water savings for farmers without compromising primary productivity of crop plants. While there are many ways in which this study differs from Baguskas et al. (2018), an important distinction is that we compared how coastal fog events affect carbon, water, and radiation fluxes using eddy covariance side-by-side with canopy-scale flux measurements. Determining if patterns at the level of canopies (m^2) are consistent with the agroecosystem scale (>100 m^2) has greater potential to increase farmer confidence to adjust their irrigation regime based on knowledge of local meteorology.

Coastal fog enshrouds California predominately during the rainless summertime months (May–August) and impacts the water, carbon, and energy balance of ecosystems in several ways (Weathers et al., 2020). Fog-drip can directly augment plant water availability by increasing soil moisture in forests (Baguskas et al., 2017; Carbone et al., 2013; Dawson, 1998; del-Val et al., 2006; Ewing et al., 2009; Fischer et al., 2009), shrublands (Vasey et al., 2012), and grasslands (Corbin et al., 2005). Lower ambient temperature and higher relative humidity during fog events dampen atmospheric water stress and reduce transpiration rates, thus plant demand for water (Baguskas et al., 2016, 2018; Burgess & Dawson, 2004; Johnson & Smith, 2008; Ritter et al., 2009). Shading by coastal fog reduces total incoming solar radiation and evaporative water loss from ecosystems (Fischer et al., 2009), which impacts plant and microbial activity (Carbone et al., 2013). Coastal fog also changes the quality of plant-available light (Johnson & Smith, 2008; Letts & Mulligan, 2005; Reinhardt et al., 2010). The change in light quality and availability can be important in non-forested ecosystems, too. Baguskas et al. (2018) demonstrated that leaf-level photosynthesis of strawberry crops in coastal California was reduced by 30% during foggy compared to clear-sky conditions. While the decline of individual leaf photosynthesis can be attributed to lower plant-available light during fog events, studies have also shown that primary productivity, namely gross primary productivity (GPP), can increase on cloudy days at larger spatial scales (Still et al., 2009; Wu et al., 2012; Zhang et al., 2011). A primary explanatory factor of this pattern is greater diffuse sky irradiance, that is, scattered light, that drives higher plant light-use efficiency (LUE), unit of carbon gained per photon of light absorbed (Alton et al., 2007; Gu et al., 2003; Still et al., 2009; Williams et al., 2014), including in croplands (Cheng et al., 2014; Choudhury, 2001).

Diffuse photosynthetically active radiation (PAR_D) increases as a proportion of total PAR when incoming shortwave radiation is scattered by cloud cover (Oliphant et al., 2011), airborne particulate matter emitted by volcanic eruptions (Gu et al., 2003), wildfires (Hemes et al., 2020), dust storms (Xi & Sokolik, 2012), and/or aerosols from anthropogenic emissions (Jacovides et al., 1997). Ecosystem GPP increases under diffuse light conditions because leaves that are deeply shaded under direct beam light receive higher photon density under diffuse light conditions (Alton et al., 2007; Still et al., 2009). Cheng et al. (2014) found that PAR_D explained 41% of the variation in cropland GPP independent of direct light levels. Enhanced LUE in response to greater PAR_D has been demonstrated in numerous ecosystems, including coniferous and broadleaf forests (Cheng et al., 2014; Oliphant et al. 2011; Still et al., 2009), arctic tundra (Williams et al., 2014), wetlands (Hemes et al., 2020), and agriculture (Choudhury, 2001; Hemes et al., 2020). However, the strength of this relationship depends on the specific sky conditions. For example, optically thin clouds or aerosols that enhance intermediate levels of PAR_D resulted in a net increase in annual GPP for a mixed deciduous forest, while optically thick clouds had a negative impact on GPP (Oliphant et al., 2011). In this study, the trade-off between the benefit of diffuse light enhancing crop LUE and the reduction of total PAR by clouds that dampen GPP will depend on the characteristics of the fog event.

Detecting and characterizing spatial and temporal patterns of coastal fog in ecologically significant ways necessitates the coupling of ground and remotely sensed observations (Rastogi et al., 2016). Using a spatially explicit model, Clemesha et al. (2016) investigated the long-term seasonal patterns of coastal low cloudiness (CLC) during the summertime and found that in comparison to southern California, cloud cover in central/northern California peaks later in summer. The extent and duration of coastal fog events in California is inversely related to urbanization based on an analysis combining airport observations of air temperature and coastal fog (Williams, Schwartz, et al., 2015). Torregrosa et al. (2016) used Geostationary Operational Environmental Satellite (GOES) products to develop fog and low cloud frequency maps that quantify spatial patterns of coastal fog during the daytime and nighttime at hourly, seasonal, and decadal time steps in California, which can be used to predict how changes in coastal fog have or will impact bioclimates important for species' distribution. In California's Central Valley, Baldocchi and Waller (2014) found a decline in winter fog over a 32-year period based on analysis of spatial and temporal patterns of fog climatologies. A decline in winter fog has negative implications for the fruit and nut tree yields in the region (Baldocchi & Waller, 2014). These studies show how remote sensing approaches can be used to quantify fog dynamics that can impact surface conditions in ecologically meaningful ways. What remains unclear is how spatio-temporal variation in fog frequency directly impacts agroecological patterns and processes, such as primary productivity of crops.

The objectives of our study were to: (1) link remote sensing with ground-based radiation flux observations for detecting, characterizing, and quantifying fog events, and (2) compare carbon, water, and energy fluxes in strawberry crops over space and time in the presence and absence of coastal fog. We hypothesized that: (1) downwelling longwave radiation ($L\downarrow$), a component of Earth's radiation balance, would be a reliable ground-based measurement for detecting and characterizing coastal fog because $L\downarrow$ magnitudes should be significantly greater under low clouds due to their higher emissivity than clear-skies; (2) $L\downarrow$ would relate to cloud albedo observed from satellite imagery; (3) crop LUE would increase under foggy conditions due to the enhancement of diffuse light; and (4) crop water-use efficiency would increase under foggy conditions in response to a combination of lower atmospheric evaporative demand and higher LUE. To test our hypotheses, we quantified carbon gain and water loss of strawberry crops on a large, conventional farm in central coastal California at the canopy (1 m^2) and field (>100–300 m^2) scales and linked them to temporal variation in fog events during the growing season (May–October 2016).

2. Materials and Methods

2.1. Study Site

We conducted a field investigation at a coastal, conventional strawberry farm located in the Salinas Valley, California. The farm was 0.25 km^2 in area and located approximately 1.5 km from the coastline near sea level (see Baguskas et al., 2018 for site map). The peak strawberry growing and harvest season began in May 2016 and the final harvest was in October 2016. The strawberry crops (*Fragaria* × Albion var.) were grown using conventional methods (Fissell, 2018). Strawberry rhizomes were planted in parallel rows on top of

field beds. Each strawberry bed (52 cm wide and 30 cm tall) was planted with two rows of strawberry plants that were spaced 30 cm apart. A layer of dark gray-colored plastic mulch was used to cover the soil surface per local agricultural practices. Two drip irrigation tapes were placed in each bed beneath the plastic mulch close to the strawberry plants, and were used to water the crop during the entire growing season. Each irrigation event usually occurred between 08:30 and 10:30 h and was applied at 9 psi for ~1.5 h. We measured irrigation flow rates by installing a flowmeter (Badger Flow Meter, Meter Group Inc.) in four beds where we sampled and soil moisture sensors (EC5, Meter Group Inc.) at three depths (~5, 10, and 20 cm). We found that strawberry plants were irrigated regularly during the growing season, which maintained soil volumetric water content in the primary rooting zone (~10–20 cm deep) at nearly 0.25 m^3 m^{-3} (Figure S1). In other words, plants were well-watered with the irrigation treatment, and we were focusing on the atmospheric impacts of fog and energy budgets.

2.2. Quantifying Coastal Fog and Meteorology

2.2.1. Remote Sensing of Coastal Fog

We used GOES-WEST 15 Imager measurements to identify and quantify cloudiness. As in our previous work (Baguskas et al., 2018), we used the visible, shortwave infrared (IR), longwave IR channels (channel numbers 1, 2, and 4, respectively) and an established algorithm (Clemesha et al., 2016) to identify the presence of low-level water clouds (as distinct from clear conditions and high-level ice clouds) at 4 km resolution every 30 min over a 24 h time period. The percent of time that low-level clouds were detected in the satellite data is referred to as the coastal low cloud and fog (CLCF) index and is summarized with monthly means for June–August 2016. Albedo is a measure of reflectivity, defined as the ratio of reflected radiation to incident radiation. We used GOES total scene albedo measurements at the 4 km grid scale co-located with the study site every 30 min during daylight hours (07:00–18:30 h) to quantify sky conditions. If cloud cover and/or cloud optical thickness increases within a pixel, the value of albedo increases in that pixel. We used total GOES albedo to provide a scale of cloud reflectivity, that is, how much sunlight the cloud is blocking from reaching the surface, and related the albedo scale to radiation metrics recorded on the ground using a pyrgeometer.

2.2.2. Measuring Local Coastal Fog and Meteorology

We refer to "foggy" conditions as the presence of a low-level stratiform cloud layer either in contact with the ground or elevated above it. Non-foggy conditions refer to clear-sky conditions. Williams, Schwartz, et al. (2015) use altitudinal variation in cloud base height (CBH) to distinguish fog and low stratus clouds in coastal California, where the lowest 25% of stratus are defined as "fog" and low stratus clouds are between the "fog" altitude and 1,000 m. Any clouds above 1,000 m are defined as high clouds. Using this definition, we found that clouds in our study area with CBHs at or below 175 m were "fog" and clouds with CBHs between 175 and 1,000 m were low stratus clouds. Hereafter, we use "coastal fog" or "foggy" conditions to refer to both fog and low stratus clouds. Using airport cloud height observations to assess the frequency of coastal fog events versus high clouds, we found that high clouds occurred less than 5% of the time during our study period. Therefore, coastal fog was the dominant cloud type during our study period (Figure S2 and Table S1). We found that a threshold value of downwelling longwave radiation was useful to distinguish foggy and non-foggy conditions, which is described in our results section.

We installed a passive fog collector (Hiatt et al., 2012; Schemenauer & Cereceda, 1994) at approximately 0.30 km from our field site to measure total fog water inputs at hourly intervals (Baguskas et al., 2018). The fog collector was constructed of a 1 m^2 mesh screen mounted 2 m off the ground surface perpendicular to the prevailing wind direction. Fog water droplets deposited on the mesh screen drip into a collection trough below that is angled toward a tipping bucket rain gauge (ECRN-100 high-resolution rain gauge, Meter Group Inc.). Each tip of the tipping bucket is equal to 0.2 mm of water. The total number of bucket tips was recorded every 15 min for the entire study period. We calculated the total fog water inputs each hour of the day (Baguskas et al., 2018). Meteorological observations that were co-located with the passive fog collector included: leaf wetness (mV) (Leaf Wetness Sensor, Meter Group Inc.), temperature (°C) and relative humidity (%) (VP3, Meter Group Inc.), total solar radiation (W m^{-2}) (PYR, Meter Group Inc.), and wind speed, direction, and gust speed (DS2-Sonic Anemometer, Meter Group Inc.). Each environmental

variable was recorded every 15 min over the study period. We summarized these data by calculating the hourly average value for each variable. These meteorological measurements supplemented the eddy covariance observations by providing information about whether or not fog events generated drip, which allowed us to disentangle variation in coastal fog events.

2.3. Micrometeorological Measurements

We deployed a micrometeorological station in the strawberry farm between June 10 and October 3, 2016, including eddy covariance (EC) instruments to measure trace gas fluxes of CO_2 and H_2O. The location of the station was selected to ensure reasonable fetch of homogeneous strawberry fields during the prevailing onshore air flows ranging from SW to NW. The eddy covariance system was comprised of a 3-dimensional sonic anemometer-thermometer (CSAT3, Campbell Sci.) and an open path infrared gas analyzer (Li-7500, LiCor Inc.), which were deployed at 3.0 m above ground level. These instruments were sampled at 10 Hz by a CR1000 data logger (Campbell Sci.) and stored on a flash memory card. The major components of the surface radiation budget were measured using a four-component radiometer (CNR1, Kipp&Zonen) deployed at 0.5 m above the strawberry canopy. This provided incident global solar radiation, the portion reflected upward from the crop canopy and longwave radiation (instrument spectral response is 5–50 μm), both downwelling from the atmosphere above, and emitted from the upper surfaces of the strawberry crop canopy. The instrument is widely used by the micrometeorological and biometeorological community and has been used for global estimates of atmospheric downward longwave radiation for land surfaces (e.g., Wang & Liang, 2009). Air temperature and relative humidity were measured at 3.0 m using a HMP45C probe (Vaisala Corp.), and soil heat flux was determined using three heat flux plates (HF01, Hukseflux) installed at 6 cm with soil temperature in the layer above measured by three sets of spatial averaging thermocouples. Implausible spikes in the high frequency data set were defined by three or fewer consecutive samples greater than 3.5 standard deviations of a moving 5-min window (after Vickers & Mahrt, 1997). Vertical fluxes were calculated from 30-min covariance blocks after removal of these spikes in the high frequency data. The CO_2 and H_2O mass fluxes were then corrected for density fluctuations (WPL corrections), and planar-fit coordinate rotations were applied (Lee et al., 2004). The distribution of the flux source area in the upwind direction was calculated for each 30-min period ($n = 6{,}995$) using the analytical footprint model of Hsieh (2000). Over the entire study period, the 90th percentile of the flux source in the upwind direction ranged from a few meters to more than 600 m, though averaged 157 m, with a median of 89 m. This data set of gas fluxes, therefore, spatially represents fields of strawberry crop rows over an area of approximately 0.5–3 hectares.

Eddy covariance data quality control included data flagging dependent on instrument performance, flux source area and turbulent conditions. First, data were flagged based on diagnostic codes for the sonic anemometer and gas analyzer, although the number of periods rejected due to instrument performance was negligible. Second, using a satellite image of the farm, the distance from the tower to the boundary of homogenous strawberry fields was determined for each octant of wind direction. These distances were compared with those found using the source area model, and data were rejected if less than 90% of the flux source area was contained within the strawberry fields. Due to this criterion, 16% of 30-min observational periods were rejected, although only 9% during daylight hours when less stable atmospheric conditions shorten the fetch. EC measurements have been shown to underestimate the flux under conditions of low turbulent energy, which particularly occurs at night (Lee et al., 2004). Following Papale et al. (2006), we estimated the minimum friction velocity (u^*) threshold for rejection for this site as $u^* \leq 0.1$ m s^{-1}. This criterion caused the most frequent rejection of data (18% over the entire study period and 9% during daylight hours).

The EC-determined net ecosystem exchange of CO_2 (NEE, mgC m^{-2} s^{-1}) is the balance between gross primary production by photosynthesis and ecosystem respiration (R_E). The sign convention used here is that negative NEE represents an atmosphere to ecosystem flux while positive NEE represents an ecosystem to atmosphere flux. The relative contributions of GPP and R_E to an eddy covariance measurement of NEE were estimated following (Lee et al., 2004), by modeling respiration based on the relationship between soil temperature and nocturnal NEE at the 30-min timescale (assuming photosynthesis is zero at night). This was done separately for each month to account for changes in the phenological cycle. Based on this relationship, we modeled R_E for each daytime period and GPP was calculated by $GPP = NEE + R_E$.

We fit a commonly used empirical light use efficiency model based on a rectangular hyperbola (Equation 1) to the observed PAR and GPP estimates at the 30-min timescale (e.g., Gilmanov et al., 2010; Oliphant et al., 2011; Xu & Baldocchi, 2004),

$$\mathrm{GPP} = \frac{\alpha \times A_{\max} \times \mathrm{PAR}}{A_{\max} + \alpha \times \mathrm{PAR}} \quad (1)$$

where the coefficient α is the initial slope of the LUE curve and A_{max} is the point of maximum GPP.

In order to estimate the diffuse fraction of PAR (ϕ), we used a semi-empirical model that requires only total solar radiation ($K\downarrow$) to be measured (Oliphant & Stoy, 2018). First, global PAR was calculated from $K\downarrow$ using a regression derived from a coastal San Francisco location which used the same pyranometer as this study (PAR = 2.14 $K\downarrow$, $r^2 = 0.998$, $n = 62{,}417$). Second, the equivalent extraterrestrial solar radiation (K_{Ex}) was calculated for each 30-min period using Whiteman and Allwine (1986), and the transmission index was derived from $\tau = K\downarrow/K_{Ex}$. Third, τ was used to estimate ϕ by,

$$\text{for } \tau < 0.42; \phi = 0.97, \text{for } 0.42 < \tau < 0.78\, \phi = A^0 + A^1\tau, \text{and for } \tau > 0.78; \phi = 0.17,$$

$$\text{where } A_1 = \frac{\phi_1 - \phi_0}{\tau_1 - \tau_0} \text{ and } A_0 = \phi_1 - A_1\tau_1. \quad (2)$$

Model coefficients were derived for summer months from radiation datasets that included diffuse PAR data collected at two nearby coastal sites (Oliphant et al., 2021). To assess the relationship between GPP, PAR, and ϕ, we calculated average GPP for every 100 μmol m^{-2} s^{-1} bin of PAR and 0.1 bin of ϕ, creating a matrix of GPP values for each PAR-ϕ combination. This was smoothed using a 2-D convolution, whereby the value for each point in the matrix is the weighted average of the point itself (60%) and the surrounding eight points (5% each), and created a filled contour plot of the derived matrix. A Pearson correlation analysis was performed to test relationships between field measurements of micrometeorology and $L\downarrow$ with daytime GOES albedo (n = 2,408 observations). This analysis was performed using the 'stats' package in R version 3.6.1.

2.4. Canopy Physiology

We evaluated the physiology of strawberry plants at the canopy scale (0.6 m^2) to foggy and non-foggy conditions within the areal footprint of the EC-tower (approximately 0.5–3 hectares) by measuring CO_2 and H_2O vapor fluxes. We randomly sampled canopy height and leaf area index (LAI; Model LI-2200, LI-COR) from 30 to 35 strawberry plants in mid-July. Average canopy height was 32 ± 3.12 cm (n = 30) at full-leaf emergence with an average LAI of 1.76 ± 0.46 (n = 35) and range between 1.13 and 3. We used an open-path infrared gas analyzer (IRGA; Model LI-7500A, LI-COR) placed in an infrared-transparent Tefzel® chamber (DuPont; 0.75 m wide × 0.75 m long × 0.75 m tall) over four plant canopies per flux measurement, as described in our previous work (Baguskas et al., 2018). We randomly collected approximately 10 canopy flux measurements per day between 09:00 and 13:00 h from mid-June to late-August in 2016. The concentration of CO_2 and H_2O were recorded once per second over approximately 300 s (5 min) per sample. Change in concentration (mg m^{-3} s^{-1}) of gases measured in the chamber were converted to a flux (μmol m^{-2} canopy area s^{-1}) (Baguskas et al., 2018; Patrick et al., 2007). To normalize canopy-level CO_2 and H_2O flux measurements by canopy area, we measured ground area per sample from a digital photograph of the four plant canopies at 1 m overhead, which was converted to a binary image from which fractional green canopy cover was calculated using the Canopeo App (Patrignani & Ochsner, 2015). We define canopy-level carbon uptake as Net Canopy Exchange (NCE), which is net ecosystem exchange with the soil component reduced due to the agronomic practice of covering strawberry soils with plastic. Similarly, soil evaporation and respiration were excluded from our canopy-level CO_2 and H_2O flux measurements. Canopy-level water-use efficiency (WUE) and LUE were calculated by dividing NCE (μmol CO_2 m^{-2} s^{-1}) by water vapor conductance (mmol H_2O m^{-2} s^{-1}) and photosynthetically active radiation (PAR, μmol m^{-2} s^{-1}), respectively. An analysis of variance was performed to test for statistical differences in physiological responses at the canopy-level

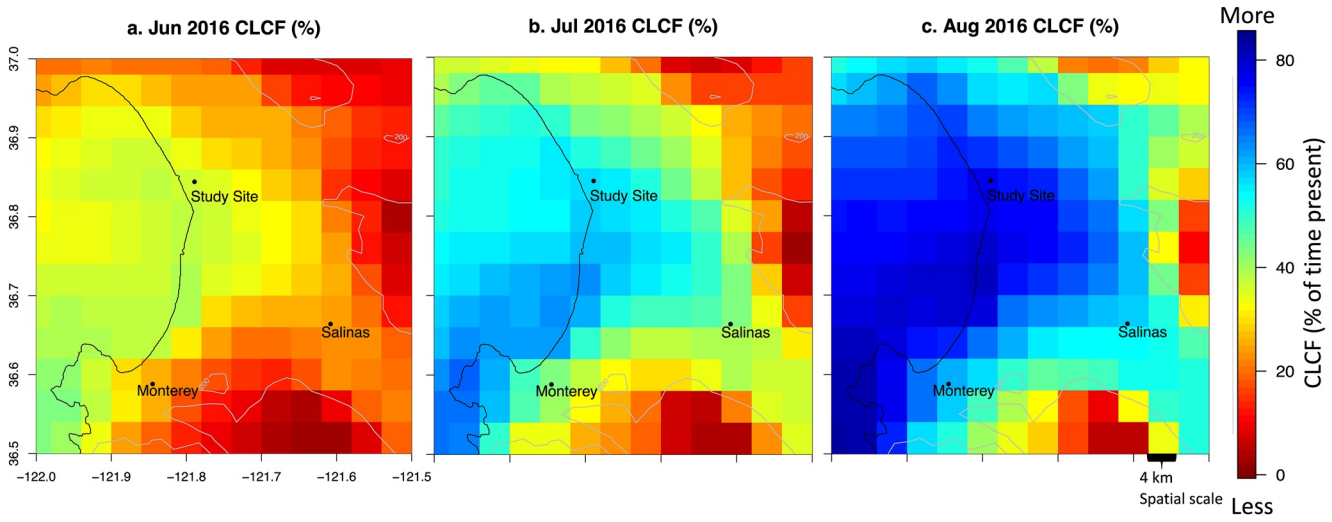

Figure 1. (a)–(c) Monthly coastal low cloudiness and fog (CLCF) index for the study area calculated from GOES-satellite imagery. The scale varies from lower (red) to higher (blue) occupancy by CLCF during June (a), July (b), and August (c). Black dots represent our study site in the Monterey Bay, the Salinas Municipal airport, and Monterey Regional airport (airport observations are used in supporting information). Dark gray line demarks 200 m elevation contour. CLCF, coastal low cloudiness and fog; GOES, Geostationary Operational Environmental Satellite.

between foggy (n = 80) and non-foggy (n = 63) conditions using the "aov" function in RStudio version 0.99.892 (R Development Core Team 2016) statistical software package.

3. Results

3.1. Characterizing Coastal Fog Events From Remote Sensing, Microclimate Variables, and Ground-Based Radiometers

At our study site, average monthly satellite-derived CLCF increased progressively during the summer months. CLCF were present during 38% of June, 57% of July, and 76% of August (Figures 1a–1c). Based on ground observations from mid-July (DOY 201) to early August (DOY 220), $L\downarrow$ values increased by 24% from clear-sky to foggy conditions at the onset of a fog-drip event (Figures 2a and 2b, and I to II). After the fog-drip event, $L\downarrow$ values remained high (~380 W m^{-2}) between DOY 213–220 (Figures 2a and 2b, III, fog and low cloud). Total direct photosynthetically active radiation (PAR_S, 400–700 nm, μmol m^{-2} s^{-1}) decreased by 50% between clear and foggy conditions, while diffuse PAR (PAR_D) increased by 80% (Figures 2c and 2d, I to III). Vapor pressure deficit (VPD, kPa) declined by approximately 75% between the clear-sky conditions and fog-drip event (Figure 2e).

We observed a bimodal distribution in the frequency of $L\downarrow$ during the summertime (Figure 3). Non-foggy conditions were characterized by $L\downarrow$ values between 250 and 350 W m^{-2} (e.g., $L\downarrow$ = 309 W m^{-2}) while values between 350 and 400 W m^{-2} characterized foggy conditions (e.g., $L\downarrow$ = 380 W m^{-2}) (Figure 3). We used a $L\downarrow$ threshold value of 350 W m^{-2} to distinguish foggy and non-foggy conditions based on the minimum frequency between the two dominant modes in the distribution. We found that $L\downarrow$ was a useful indicator of when there are clouds above the field site, regardless of specific cloud base height value (Figure S2). However, coastal fog events were the dominant cloud type during the study period, as compared to high clouds (Figure S2 and Table S1). We also found that GOES-derived total albedo predicts $L\downarrow$ values less than 350 W m^{-2} corresponding to non-foggy conditions, whereas $L\downarrow$ values above 350 W m^{-2} correspond to foggy conditions (Figure S3). Based on this $L\downarrow$ threshold, we found that it was foggy 55% and not foggy 44% of the 30-min periods during the summer, regardless of fog-drip events (Figure 3).

GOES-derived total albedo, a good proxy for daytime CLCF, is strongly and positively correlated with $L\downarrow$ (r = 0.83, P < 0.01) (Figure S4), which is also evident in the timeseries of $L\downarrow$ and GOES albedo (Figure S5). GOES-derived total albedo is also positively correlated with diffuse fraction of PAR (ϕ; r = 0.83, P < 0.01) and relative humidity (RH; r = 0.54, P < 0.01) measured from the eddy covariance tower (Figure S4). Total

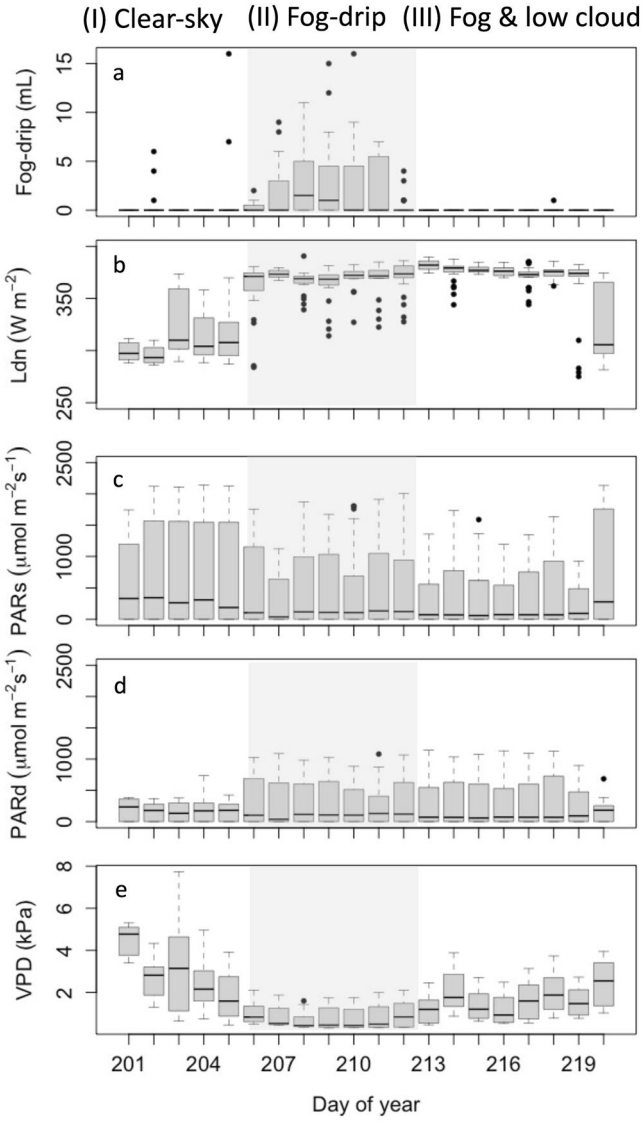

Figure 2. Micrometeorological conditions of a fog event. Fog-drip magnitude (a), downwelling longwave radiation (b), direct photosynthetically active radiation (c), diffuse photosynthetically active radiation (d), and vapor pressure deficit (e) during 2016 DOY 201–219. The fog event is separated into clear-sky conditions (I), a fog-drip event of several days (II), and eight fog & low cloud days (III).

albedo is linearly and inversely correlated with $K\downarrow$ ($r = -0.70$, $P < 0.01$). During fog events, more solar radiation is reflected from the top of clouds (and a smaller fraction absorbed by clouds) and $K\downarrow$ scales and decreases accordingly. Total albedo had a weak, negative correlation to GPP ($r = -0.23$) but a stronger, negative relationship to evapotranspiration rates (ET; $r = -0.57$) (Figure S4).

3.2. Crop Response to Fog

3.2.1. Strawberry Field Water-Use and Light-Use Efficiency Increase During Fog Events

Diurnal 30-min averages over the growing season show lower total PAR during foggy than non-foggy conditions (Figure 4a). Despite 45% lower light levels at the daily timescale, we observed similar rates of GPP and NEE for strawberry plants under foggy and non-foggy conditions (Figures 4b and 4c and Table 1a). Conversely, evapotranspiration rates (ET, mm) were consistently lower (overall by 39%) during foggy than non-foggy periods (Figure 4d). Together, WUE of strawberry crops was 50% higher during fog events (Table 1a), which is also evident from the steeper initial rate of change in GPP with ET during foggy ($\alpha = 30.8$) than non-foggy ($\alpha = 22$) conditions, and much higher A_{max} (Figure 5a; Table 1a). The curvilinear fit (r-squared values) for determining WUE was higher under foggy than non-foggy conditions (Table 1a). The difference in fit is likely related to the wider range of microclimate variables (especially downwelling shortwave radiation, ambient temperature, and VPD) experienced under non-foggy compared to foggy periods. During foggy periods, conditions tend to be more consistent, that is, low light, smaller range in temperature (~12°–15°C) and low VPD. These results show that strawberry plants transpire less water per unit carbon gained during fog events compared to non-foggy conditions. Since these plants were equally well-watered throughout the growing season, lack of plant water availability cannot explain these patterns.

Field-scale strawberry crop LUE was higher during fog events as shown by the initial slope of the curvilinear relationship fit between GPP and PAR, which was nearly twice as steep during foggy ($\alpha = 0.0395$) than non-foggy ($\alpha = 0.0210$) conditions (Figure 5b; Table 1b). The curvilinear fit (r-squared values) for determining LUE was higher under foggy ($R^2 = 0.72$) than non-foggy ($R^2 = 0.44$) conditions (Table 1b). Figure 6 shows GPP as a function of both PAR and the diffuse fraction of PAR (ϕ). GPP was positively correlated with PAR as expected. However, for a given level of PAR, GPP was also positively correlated with the fraction of diffuse PAR (ϕ) (Figure 6). The optimal light conditions for GPP were at moderately high PAR levels (~1,500 μmol m^{-2} s^{-1}) when the diffuse fraction was also moderately high (ϕ = ~0.7).

3.2.2. Strawberry Canopy Water-Use and Light-Use Efficiency Increase During Fog Events

NCE was slightly higher, i.e., more negative, on non-foggy than foggy days (Figure 7a; average difference in NCE of 2 μmol m^{-2} s^{-1}; $F = 4.4$, $P = 0.04$). Canopy transpiration rates were significantly lower on foggy compared to non-foggy periods (Figure 7b; $F = 27.3$, $P < 0.001$). Consistent with field-scale observations, canopy-scale strawberry plant water-use efficiency was 32% higher during foggy compared to non-foggy periods, and this difference was significant (Figure 7c; $F = 5.7$, $P = 0.02$). We also found a significant correlation between canopy-scale transpiration rates and field-scale evapotranspiration rates ($r = 0.47$, $P < 0.001$), suggesting that mechanisms that control leaf and canopy transpiration rates can determine water loss at

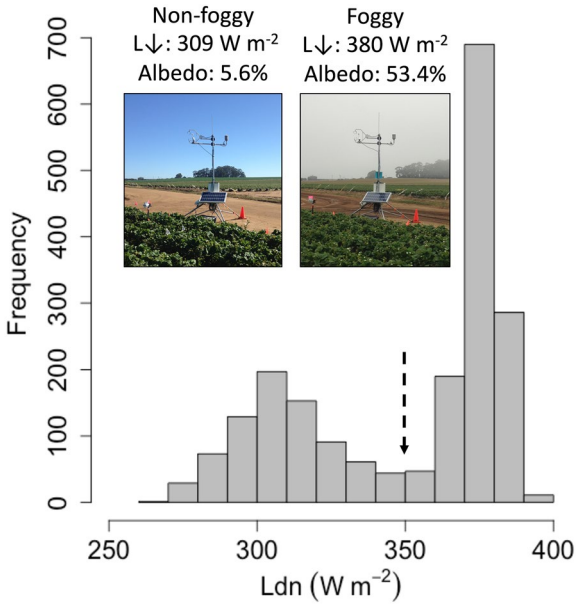

Figure 3. Frequency distribution of the total number of observations of downwelling longwave radiation ($L\downarrow$ for wavelengths between 4.5 and 52 μm, W m^{-2}) observed over the summertime (DOY 162–246). Each bar represents the total number of $L\downarrow$ observations within each 10 W m^{-2} increment. Over the sampling period, there were a total of 1,177 h of fog and 825 h of non-foggy conditions. Photographs from the field site show conditions during a (left) clear-sky and (right) foggy day with corresponding values of $L\downarrow$ and total GOES albedo (% of reflected radiation to incident radiation) above each image. Vertical dashed line indicates an $L\downarrow$ threshold of 350 W m^{-2} that separates non-foggy ($L\downarrow < 350$ W m^{-2}) and foggy ($L\downarrow > 350$ W m^{-2}) conditions. GOES, Geostationary Operational Environmental Satellite.

the field-scale. Canopy light-use efficiency was also significantly higher by 68% during foggy compared to non-foggy periods (Figure 7d; $F = 36.9$, $P < 0.001$).

4. Discussion

4.1. Significant Increase in Crop Water and Light-Use Efficiency During Coastal Fog Events

Our results support our third and fourth hypotheses that strawberry crops would have higher LUE and WUE during summer coastal fog events compared to clear-sky days. The increase in strawberry crop WUE during fog events was consistent with patterns observed in the previous year (Baguskas et al., 2018). These findings support the idea that including local meteorology in water-use decisions can be aligned with water conservation goals in California's water-stressed agricultural systems. For example, in these strawberry fields irrigation application could be reduced during foggy periods, especially during drought years. Specifically, since WUE of strawberry crops doubles during foggy compared to clear-sky conditions, it is plausible for farmers to reduce irrigation by approximately half. A more conservative and likely realistic adjustment to irrigation during fog events would be a reduction by 25%, and this is supported not only based on the increase in crop WUE but also the effect of irrigation on volumetric soil moisture (Figure S1).

Similar rates of carbon uptake between foggy and non-foggy conditions could be explained by greater LUE of crops observed at both the canopy and field-scales. The increase in LUE during fog events is consistent with numerous studies that have investigated the impact of cloudiness on ecosystem carbon fluxes (Alton et al., 2007; Berry & Goldsmith, 2020; Cheng et al., 2014; Choudhury, 2001; Emmel et al., 2020; Kanniah et al., 2013; Oliphant et al., 2011; Williams et al., 2014). Specifically, the initial light response (α) that we observed for strawberry crops was higher under diffuse than direct light conditions, and agrees with findings across at least six other crop types (Emmel et al., 2020). We showed that highest GPP occurred under conditions when both total PAR and ϕ were moderately high, which likely occurred under conditions of thin clouds when most light was able to penetrate the canopy but when there was also a high degree of scattering. This suggests that maximum carbon uptake by strawberry crops may be greatest at the transition between foggy and clear-sky conditions, which tends to be in the late-morning and afternoon. Similarly, Hemes et al. (2020) found that gross ecosystem productivity (GEP) over croplands in the Central Valley of California was sensitive to the ratio of PAR_S and PAR_D as affected by wildfire smoke. On more extreme smoke days, GEP declined in response to lower total PAR while on moderate smoke days, GEP increased in response to higher LUE of crops. Alton et al. (2008) determined that carbon sequestration rates do not increase during overcast versus clear-sky conditions, emphasizing that the direction and magnitude by which diffuse light impacts ecosystem productivity varies across ecosystem types and cloud fraction or thickness. The results from this study suggests strawberry crops also experience a photosynthesis trade-off produced by clouds which both limit available light for photosynthesis and enhance light use-efficiency. In the case of coastal fog over strawberry crops, the trade-off produces very similar levels of photosynthesis under clear skies and foggy conditions at the field scale.

We hypothesized that a primary mechanism underlying enhanced LUE of strawberry crops during fog events is the change in geometry of the incident light, such that diffuse light irradiates more leaves within the canopy than direct-beam radiation. This could effectively elevate whole-plant carbon uptake (Farquhar & Roderick, 2003). Emmel et al. (2020) demonstrate that GPP was significantly greater under diffuse rather than direct radiation conditions for six different arable crops, which varied in their canopy structures. Canopy architecture variables, such as mean leaf tilt angle, were most important under diffuse conditions relative to climate factors that contributed more explanatory power to variation in GPP under direct light

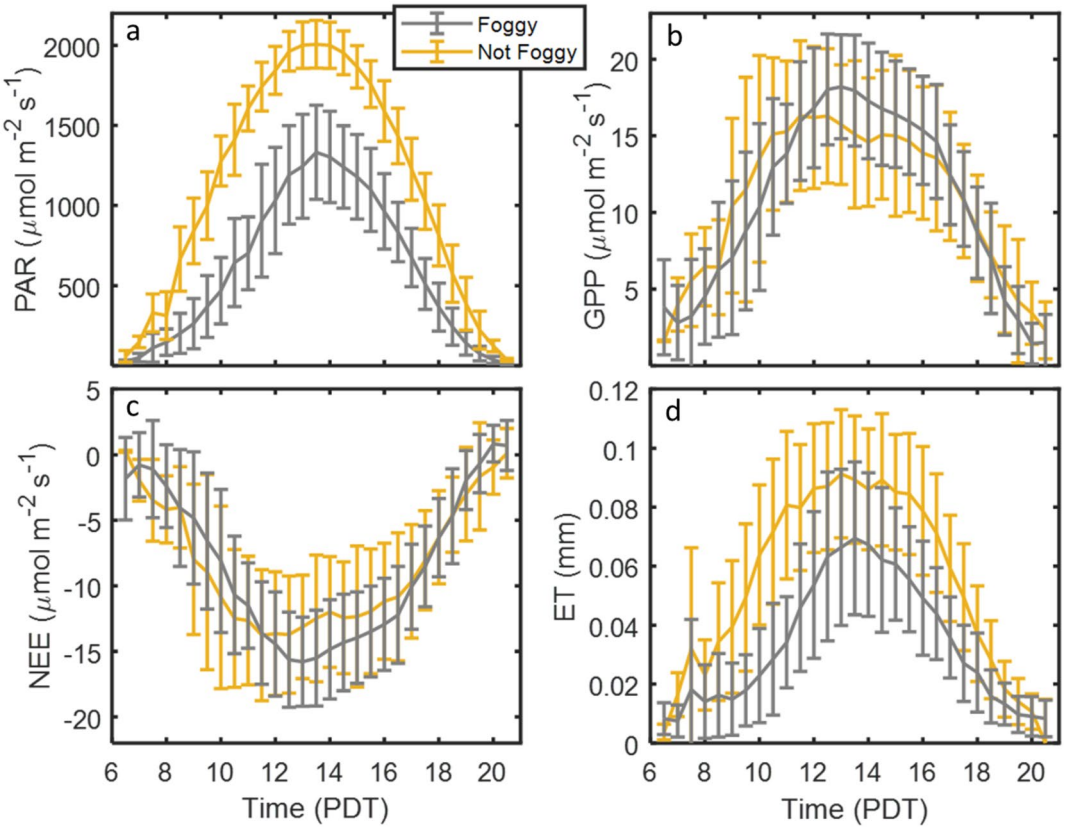

Figure 4. Diurnal 30-min average and standard deviation (error bars) of (a) PAR, (b) GPP, (c) NEE, and (d) ET for foggy (gray) and non-foggy (orange) conditions from June to September 2016 determined by eddy covariance for strawberry crops at the field scale (0.5–3 ha). ET, evapotranspiration; GPP, gross primary productivity; NEE, net ecosystem exchange; PAR, photosynthetically active radiation.

Table 1
Summary of Field-Scale (0.5–3 ha) (a) Water-Use Efficiency and (b) Light-Use Efficiency Calculations Based on: Daily Totals of (a) GPP, ET, WUE and (b) GPP, PAR, LUE and Extracted Parameters From Each WUE and LUE Curves (See 5)

a. Water-use efficiency (WUE)							
	Daily totals from diurnal averages			Model coefficients and statistics			
Condition	GPP (gC m^{-2} d^{-1})	ET (kg H_2O m^{-2} d^{-1})	WUE (g kg^{-1})	α	A_{max}	R^2	N
Fog	22.9	0.97	23.6	30.8	3.6	0.57	1,137
Non-foggy	22.6	1.58	14.3	22	1.1	0.40	1,056
b. Light-use efficiency (LUE)							
	Daily totals from diurnal averages			Model coefficients and statistics			
Condition	GPP (mol m^{-2} d^{-1})	PAR (mol m^{-2} d^{-1})	LUE (mol mol^{-1})	α	A_{max}	R^2	N
Fog	1.831	31.40	0.058	0.0395	26.5	0.72	1,232
Non-foggy	1.825	57.68	0.032	0.0210	25.7	0.44	1,182

Daily totals were calculated from 30-min ensemble averages over the diurnal cycle (as presented in Figure 4) using all available observations from June to September 2016.

Abbreviations: ET, evapotranspiration; GPP, gross primary productivity; LUE, Light-Use efficiency; PAR, photosynthetically active radiation; WUE, Water-Use efficiency.

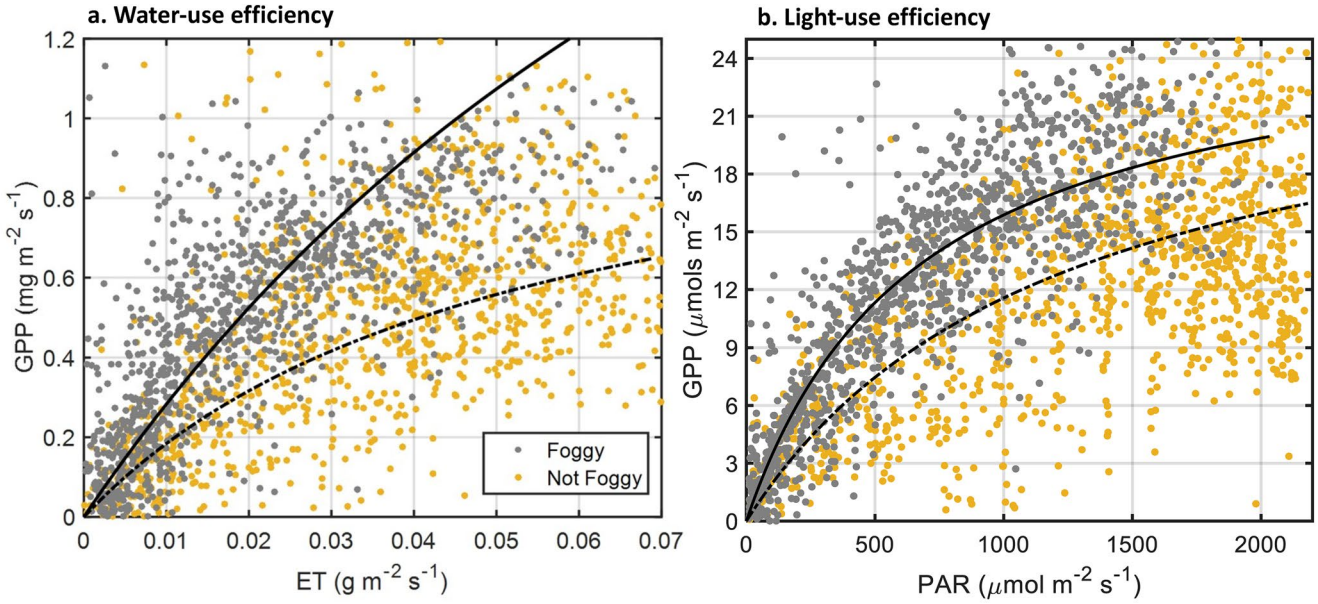

Figure 5. Field-scale (0.5–3 ha) daytime (a) water-use efficiency and (b) light-use efficiency of a strawberry field between foggy (gray) and non-foggy (orange) conditions over the growing season. Each data point represents a 30-min average between June and September 2016 from the eddy covariance tower located at our field site (n = 697, foggy; n = 504, non-foggy).

conditions. These results indicate that canopy structure is especially relevant to explain enhanced photosynthesis under diffuse light conditions.

Diffuse light penetration into the canopy is not the only mechanism we hypothesize to be involved with the enhancement of GPP under foggy conditions. For example, VPD was lower (unrelated to canopy structure), and leaf temperatures were moderated (only partly related to canopy structure) under more diffuse conditions, and these both show positive effects on ecosystem photosynthesis (e.g., Knohl & Baldocchi, 2008). In a forested ecosystem, Urban et al. (2007) attributed an observed 150% increase in ecosystem carbon uptake during cloudy days compared to clear-sky conditions to more effective penetration of diffuse radiation into the lower portion of the tree canopy. Other mechanisms could be responsible, such as more favorable microclimate conditions as well as changes in the blue/red light ratio. However, these factors explained less of the variability in NEE than the increase in diffuse light conditions (Oliphant et al. 2011; Urban et al., 2007). While an increase in PAR_D is likely the main driver of enhanced LUE of strawberry plants in our study, covarying conditions interact with changes in light scattering in ways that impact primary productivity during fog events (Fischer et al., 2009). Kanniah et al. (2013) found that the LUE of tropical savanna species was sensitive to covarying conditions during cloudy periods such that LUE increased only under favorable conditions (low temperature and VPD). Santiago and Dawson (2014) demonstrate that induction of photosynthesis by diffuse light prior to exposure to light flecks substantially increased LUE of understory plant species in coast redwood forests, especially in wetter sites where plants could maintain stomatal conductance in low light conditions. Berry and Goldsmith (2020) show that the LUE of tropical cloud forest species vary considerably under direct and diffuse light conditions, and that a species response to light is mediated by leaf wetness.

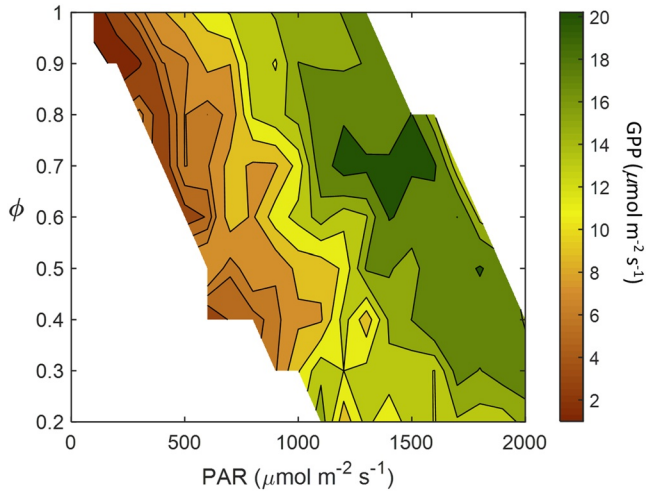

Figure 6. Field-scale (0.5–3 ha) GPP as a function of both PAR and the diffuse fraction of PAR (ϕ). White spaces to the lower left and upper right indicate where conditions do not exist, that is, extremely high PAR and highly diffuse PAR, or very low PAR and very low ϕ. PAR, photosynthetically active radiation; GPP, gross primary productivity.

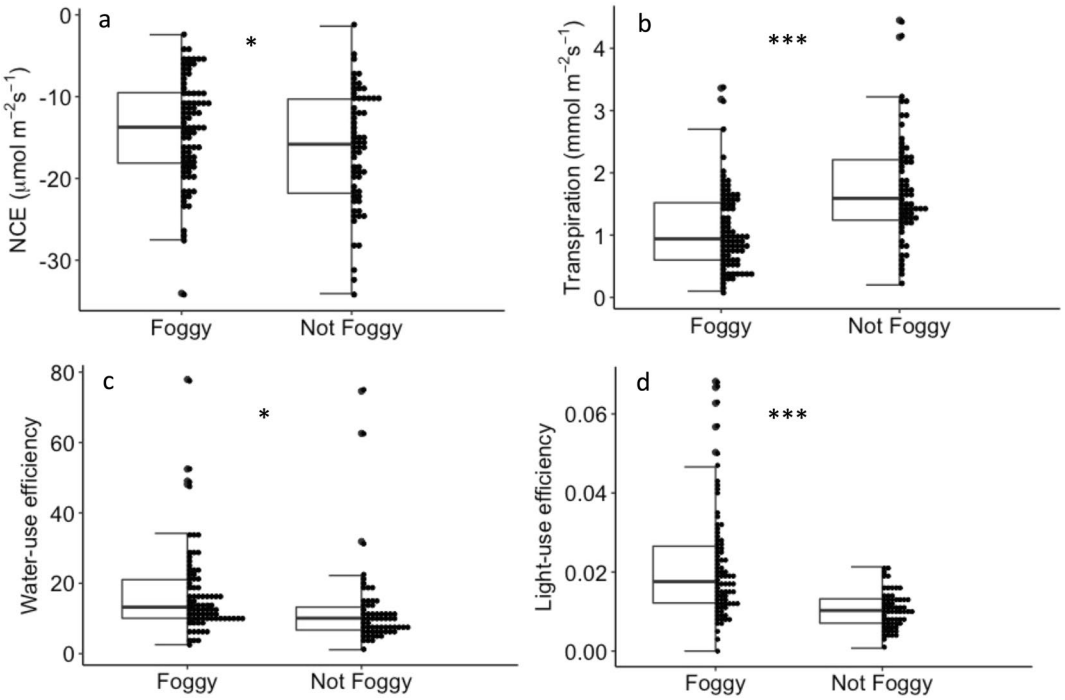

Figure 7. Canopy-scale (0.6 m^2) carbon and water vapor fluxes measured during foggy ($n = 81$) and non-foggy ($n = 63$) conditions: (a) Net canopy exchange (NCE), (b) canopy transpiration, (c) water-use efficiency (NCE Transpiration^{-1}) and (d) light-use efficiency (NCE PAR^{-1}). Asterisks indicate significant differences between foggy and non-foggy conditions ($\alpha = 0.05$; *$P < 0.05$, ***$P < 0.001$). On the left side of each box plot, the thick horizontal line is the median, the edges of the box are the 25th and 75th percentiles, the whiskers are the minimum and maximum of the data, and the points outside the whiskers are the outliers. On the right side of each box plot, points show the distribution of the data. PAR, photosynthetically active radiation; NCE, Net canopy exchange.

4.2. Identifying the Presence of Coastal Fog Using Downwelling Longwave Radiation and GOES-Derived Total Albedo

Our results support our first hypothesis that $L\downarrow$ can be used to detect low clouds associated with coastal fog events, even when there is no fog-drip. The difference in $L\downarrow$ values between foggy and clear-sky conditions (Figure 2) makes sense from a theoretical point of view. In the presence of fog, assuming an emissivity of 0.99 (Chylek & Ramaswamy, 1982) and cloud base temperatures close to air temperatures (~10°–15°C), downwelling longwave radiation would likely range from 360 to 385 W m^{-2}. Approximating a clear sky emissivity of 0.81 (Staley & Jurica, 1972), and assuming a vapor pressure of 10 hPa, $L\downarrow$ should be approximately 305–340 W m^{-2}. The distributions in Figure 3 are quite consistent with these values. Oliphant et al. (2021) found similar summertime distributions of $L\downarrow$ for other coastal California sites, with consistent differences between foggy and clear sky conditions among sites.

We determined that there is a strong and positive agreement between $L\downarrow$ and satellite-derived indices of CLCF, thus supporting our second hypothesis. The novel statistical relationship that we develop between $L\downarrow$ and GOES albedo validates the use of this satellite-derived proxy for coastal fog as a tool for investigating the ecological significance of coastal fog events, which has application in agroecosystems. We found that coastal fog events detected based on a threshold of $L\downarrow$ (for fog, $L\downarrow > 350$ W m^{-2}) influenced light conditions and micrometeorology in ways that significantly increased water-use and light-use efficiency of strawberry crops. In a coastal forest, Fischer et al. (2009) developed relationships between MODIS imagery and ground observations of shortwave radiation to show that drought stress was reduced by 20%–40% during fog events. From a methodological perspective, we demonstrate the significance of a satellite-derived index for detection of coastal fog that improves understanding of how low clouds affect the carbon, water, and energy balance of an agroecosystem.

4.3. Future of Fog and Implications for Coastal California Agriculture

California is at high risk of experiencing greater water scarcity with future droughts linked to anthropogenic warming (Diffenbaugh et al., 2015; Williams, Seager, et al., 2015), which increases farmers' vulnerability to water scarcity (Cheng et al., 2016; Fisher et al., 2017). In coastal California, extreme drought can be partially buffered by coastal fog events (Carbone et al., 2013; Fischer et al., 2009). As shown in this study and previous work (Baguskas et al., 2018), crops demand less water and water-use efficiency increases during fog events; therefore, if irrigation application is reduced on foggy days, farmers may benefit from water savings that will also help sustain agriculture in a drought-prone state. Yet, complex interactions between fog-forming processes in the atmosphere, ocean, and on land make forecasting changes in the coastal fog regime challenging and subject to a high degree of uncertainty (O'Brien et al., 2013; Torregrosa et al., 2014). That said, the number of coastal fog hours have declined in California since the early twentieth century (Johnstone & Dawson, 2010). While the future of coastal fog is uncertain, modifying current irrigation practices to include the effects of coastal fog on crop water demand will better position farmers to adapt to a potential decline of coastal fog events in the future.

5. Conclusions

In this study, we show that crop water loss is reduced and carbon gain is unchanged during summer fog events in a California agricultural system. The significant increase in crop water-use efficiency during fog events suggest that there could be water and economic savings for farmers in coastal California by modifying irrigation plans. The significant increase of light-use efficiency by strawberry crops during fog events has implications for the carbon budget of coastal agriculture. Our analyses indicate that the diffuse fraction of PAR during fog events amplifies the rate of whole-plant photosynthesis. Our findings are consistent with numerous studies that show a positive effect of diffuse light on ecosystem primary productivity from a variety of ecosystem types and at global to local scales (Gu et al., 2003).

It is a conundrum of fog research to infer surface processes using remote sensing techniques because the surface is not visible from space during fog events. Combining GOES satellite imagery and $L\downarrow$ observations, we made progress in resolving this issue. Specifically, the strong agreement between GOES total albedo and meteorological observations, namely $L\downarrow$ and diffuse PAR, that we observed increases the predictive power of satellite-derived coastal fog indices to estimate surface-atmosphere exchange of carbon, water, and energy in agricultural (and other) ecosystems during fog events.

Data Availability Statement

The data are available through Dryad Digital Repository in association with Baguskas et al. (2021). https://datadryad.org/stash/share/WKaDGB5RT-7xAjxOyjp6Zg6UfDJ7G84OWZYKn680hxo.

Acknowledgments
Funding support for this research was provided by USDA-NIFA Postdoctoral Fellowship (#2015-67012-22769). The authors would like to thank Zakery Pendleton for his excellent assistance in the field and post-processing of samples in laboratory. The authors would also like to thank Darren Blackburn for his assistance constructing the eddy covariance tower. The authors appreciate the help of Katie Birkhauser for logistical support in establishing field sites and the help of field managers and irrigators for field support. The authors would also like to thank the two anonymous reviewers for their constructive comments.

References

Alton, P. B. (2008). Reduced carbon sequestration in terrestrial ecosystems under overcast skies compared to clear skies. *Agricultural and Forest Meteorology*, *148*(10), 1641–1653. https://doi.org/10.1016/j.agrformet.2008.05.014

Alton, P. B., North, P. R., & Los, S. O. (2007). The impact of diffuse sunlight on canopy light-use efficiency, gross photosynthetic product and net ecosystem exchange in three forest biomes. *Global Change Biology*, *13*(4), 776–787. https://doi.org/10.1111/j.1365-2486.2007.01316.x

Baguskas, S. A., Clemesha, R. E. S., & Loik, M. E. (2018). Coastal low cloudiness and fog enhance crop water use efficiency in a California agricultural system. *Agricultural and Forest Meteorology*, *252*, 109–120. https://doi.org/10.1016/j.agrformet.2018.01.015

Baguskas, S. A., King, J. Y., Fischer, D. T., D'Antonio, C. M., & Still, C. J. (2017). Impact of fog drip versus fog immersion on the physiology of Bishop pine saplings. *Functional Plant Biology*, *44*(3), 339–350. https://doi.org/10.1071/FP16234

Baguskas, S. A., Oliphant, A. J., Clemesha, R. S., & Loik, M. E. (2021). Analyzing coastal fog effects on carbon and water fluxes in a California agriculutral system using approaches in biometeorology, remote sensing, and plant physiology. Dryad, data set. https://doi.org/10.5061/dryad.msbcc2fx0

Baguskas, S. A., Still, C. J., Fischer, D. T., D'Antonio, C. M., & King, J. Y. (2016). Coastal fog during summer drought improves the water status of sapling trees more than adult trees in a California pine forest. *Oecologia*, *181*(1), 137–148. https://doi.org/10.1007/s00442-016-3556-y

Baldocchi, D., & Waller, E. (2014). Winter fog is decreasing in the fruit growing region of the Central Valley of California. *Geophysical Research Letters*, *41*, 3251–3256. https://doi.org/10.1002/2014GL060018Berry

Berry, Z. C., & Goldsmith, G. R. (2020). Diffuse light and wetting differentially affect tropical tree leaf photosynthesis. *New Phytologist*, *225*(1), 143–153. https://doi.org/10.1111/nph.16121

Burgess, S. S. O., & Dawson, T. E. (2004). The contribution of fog to the water relations of Sequoia sempervirens (D. Don): Foliar uptake and prevention of dehydration. *Plant, Cell and Environment*, *27*(8), 1023–1034. https://doi.org/10.1111/j.1365-3040.2004.01207.x

California Agricultural Statistics Review. (2016). California Department of Food and Agriculture. Retrieved from www.cdfa.ca.gov/statistics

California Agricultural Statistics Review. (2019). California Department of Food and Agriculture. Retrieved from www.cdfa.ca.gov/statistics

Carbone, M. S., Park Williams, A., Ambrose, A. R., Boot, C. M., Bradley, E. S., Dawson, T. E., et al. (2013). Cloud shading and fog drip influence the metabolism of a coastal pine ecosystem. *Global Change Biology*, *19*(2), 484–497. https://doi.org/10.1111/gcb.12054

Challinor, A. J., Watson, J., Lobell, D. B., Howden, S. M., Smith, D. R., & Chhetri, N. (2014). A meta-analysis of crop yield under climate change and adaptation. *Nature Climate Change*, *4*(4), 287–291. https://doi.org/10.1038/nclimate2153

Cheng, L., Hoerling, M., Aghakouchak, A., Livneh, B., Quan, X.-W., & Eischeid, J. (2016). How has human-induced climate change affected California drought risk? *Journal of Climate*, *29*(1), 111–120. https://doi.org/10.1175/JCLI-D-15-0260.1

Cheng, S. J., Bohrer, G., Steiner, A. L., Hollinger, D. Y., Suyker, A., Phillips, R. P., & Nadelhoffer, K. J. (2014). Variations in the influence of diffuse light on gross primary productivity in temperate ecosystems. *Agricultural and Forest Meteorology*, *201*, 98–110. https://doi.org/10.1016/j.agrformet.2014.11.002

Choudhury, B. (2001). Estimating gross photosynthesis using satellite and ancillary data approach and preliminary results. *Remote Sensing of Environment*, *75*, 1–21. https://doi.org/10.1016/s0034-4257(00)00151-6

Chylek, P., & Ramaswamy, V. (1982). Simple approximation for Infrared emissivity of water clouds. *Journal of the Atmospheric Sciences*, *39*, 171–177. https://doi.org/10.1175/1520-0469(1982)039<0171:safieo>2.0.co;2

Clemesha, R. E. S., Gershunov, A., Iacobellis, S. F., Williams, A. P., & Cayan, D. R. (2016). The northward march of summer low cloudiness along the California coast. *Geophysical Research Letters*, *43*(3), 1287–1295. https://doi.org/10.1002/2015GL067081

Corbin, J. D., Thomsen, M. A., Dawson, T. E., & D'Antonio, C. M. (2005). Summer water use by California coastal prairie grasses: Fog, drought, and community composition. *Oecologia*, *145*(4), 511–521. https://doi.org/10.1007/s00442-005-0152-y

Dawson, T. E. (1998). Fog in the California redwood forest: Ecosystem inputs and use by plants. *Oecologia*, *117*(4), 476–485. https://doi.org/10.1007/s004420050683

del-Val, E., Armesto, J. J., Barbosa, O., Christie, D. A., Gutiérrez, A. G., Jones, C. G., et al. (2006). Rain forest islands in the Chilean semiarid region: Fog-dependency, ecosystem persistence and tree regeneration. *Ecosystems*, *9*(4), 598–608. https://doi.org/10.1007/s10021-006-0065-6

Deschenes, O., & Kolstad, C. (2011). Economic impacts of climate change on California agriculture. *Climatic Change*, *109*(S1), 365–386. https://doi.org/10.1007/s10584-011-0322-3

Dettinger, M., Udall, B., & Georgakakos, A. (2015). Western water and climate change. *Ecological Applications*, *25*(8), 2069–2093. https://doi.org/10.1890/15-0938.1

Diffenbaugh, N. S., Swain, D. L., & Touma, D. (2015). Anthropogenic warming has increased drought risk in California. *Proceedings of the National Academy of Sciences of the United States of America*, *112*(13), 3931–3936. https://doi.org/10.1073/pnas.1422385112

Emmel, C., D'Odorico, P., Revill, A., Hörtnagl, L., Ammann, C., Buchmann, N., & Eugster, W. (2020). Canopy photosynthesis of six major arable crops is enhanced under diffuse light due to canopy architecture. *Global Change Biology*, *26*(9), 5164–5177. https://doi.org/10.1111/gcb.15226

Ewing, H. A., Weathers, K. C., Templer, P. H., Dawson, T. E., Firestone, M. K., Elliott, A. M., & Boukili, V. K. S. (2009). Fog water and ecosystem function: Heterogeneity in a California redwood forest. *Ecosystems*, *12*(3), 417–433. https://doi.org/10.1007/s10021-009-9232-x

Farquhar, G. D., & Roderick, M. L. (2003). Atmospheric science: Pinatubo, diffuse light, and the carbon cycle. *Science*, *299*(5615), 1997–1998. https://doi.org/10.1126/science.1080681

Fischer, D. T., Still, C. J., & Williams, A. P. (2009). Significance of summer fog and overcast for drought stress and ecological functioning of coastal California endemic plant species. *Journal of Biogeography*, *36*(4), 783–799. https://doi.org/10.1111/j.1365-2699.2008.02025.x

Fisher, J. B., Melton, F., Middleton, E., Hain, C., Anderson, M., Allen, R., et al. (2017). The future of evapotranspiration: Global requirements for ecosystem functioning, carbon and climate feedbacks, agricultural management, and water resources. *Water Resources Research*, *53*, 2618–2626. https://doi.org/10.1002/2016WR020175.Received

Fissell, R. E. (2018). *California strawberry farming*. California Strawberry Commission, Retrieved from https://www.calstrawberry.com/Portals/2/Reports/Industry.Reports/Industry.Fact.Sheets/California.Strawberry.Farming.Fact.Sheet.2018.pdf.ver=2018-03-08-115600-790

Geisseler, D., & Horwath, W. R. (2016). *Strawberry production in California*. California Department of Food and Agriculture (June). Retrieved from https://apps1.cdfa.ca.gov/FertilizerResearch/docs/Strawberry_Production_CA.pdf

Gilmanov, T. G., Aires, L., Barcza, Z., Baron, V. S., Belelli, L., Beringer, J., et al. (2010). Productivity, respiration, and light-response parameters of world grassland and agroecosystems derived from flux-tower measurements. *Rangeland Ecology & Management*, *63*(1), 16–39. https://doi.org/10.2111/REM-D-09-00072.1

Gu, L., Baldocchi, D. D., Wofsy, S. C., Munger, J. W., Michalsky, J. J., Urbanski, S. P., & Boden, T. A. (2003). Response of a deciduous forest to the Mount Pinatubo eruption: Enhanced photosynthesis. *Science*, *299*, 2035–2038. https://doi.org/10.1126/science.1078366

Hemes, K. S., Verfaillie, J., & Baldocchi, D. D. (2020). Wildfire-smoke aerosols lead to increased light use efficiency among agricultural and restored wetland land uses in California's central valley. *Journal of Geophysical Research: Biogeosciences*, *125*(2), 1–21. https://doi.org/10.1029/2019JG005380

Hiatt, C., Fernandez, D., & Potter, C. (2012). Measurements of fog water deposition on the California Central Coast. *Agriculturae Conspectus Scientificus*, *02*, 525–531. https://doi.org/10.1007/s11852-016-0443-y10.4236/acs.2012.24047

Hsieh, C.-I., Katul, G., & Chi, T.-W. (2000). An approximate analytical model for footprint estimation of scalar fluxes in thermally stratified atmospheric flows. *Advances in Water Resources*, *23*(7), 765–772. https://doi.org/10.1016/S0309-1708(99)00042-1

Jackson, L. E., Wheeler, S. M., Hollander, A. D., O'Geen, A. T., Orlove, B. S., Six, J., et al. (2011). Case study on potential agricultural responses to climate change in a California landscape. *Climatic Change*, *109*(SUPPL. 1), 407–427. https://doi.org/10.1007/s10584-011-0306-3

Jacovides, C. P., Timbios, F., Asimakopoulos, D. N., & Steven, M. D. (1997). Urban aerosol and clear skies spectra for global and diffuse photosynthetically active radiation. *Agricultural and Forest Meteorology*, *87*(2–3), 91–104. https://doi.org/10.1016/S0168-1923(97)00031-2

Johnson, D. M., & Smith, W. K. (2008). Cloud immersion alters microclimate, photosynthesis and water relations in *Rhododendron catawbiense* and *Abies fraseri* seedlings in the southern Appalachian Mountains, USA. *Tree Physiology*, *28*(3), 385–392. https://doi.org/10.1093/treephys/28.3.385

Johnstone, J. A., & Dawson, T. E. (2010). Climatic context and ecological implications of summer fog decline in the coast redwood region. *Proceedings of the National Academy of Sciences*, *107*(10), 4533–4538. https://doi.org/10.1073/pnas.0915062107

Kanniah, K. D., Beringer, J., & Hutley, L. (2013). Exploring the link between clouds, radiation, and canopy productivity of tropical savannas. *Agricultural and Forest Meteorology*, *182–183*, 304–313. https://doi.org/10.1016/j.agrformet.2013.06.010

Knohl, A., & Baldocchi, D. D. (2008). Effects of diffuse radiation on canopy gas exchange processes in a forest ecosystem. *Journal of Geophysical Research*, *113*(2). https://doi.org/10.1029/2007JG000663

Lee, X., Massman, W., & Law, B. (Eds.), (2004). Handbook of micrometeorology: A guide for surface flux measurement and analysis (Vol. *29*). Springer Science & Business Media.

Letts, M. G., & Mulligan, M. (2005). The impact of light quality and leaf wetness on photosynthesis in north-west Andean tropical montane cloud forest. *Journal of Tropical Ecology*, *21*(5), 549–557. https://doi.org/10.1017/S0266467405002488

O'Brien, T. A., Sloan, L. C., Chuang, P. Y., Faloona, I. C., & Johnstone, J. A. (2013). Multidecadal simulation of coastal fog with a regional climate model. *Climate Dynamics*, *40*(11–12), 2801–2812. https://doi.org/10.1007/s00382-012-1486-x

Oliphant, A. J., Baguskas, S. A., & Fernandez, D. M. (2021). Impacts of low cloud and fog on surface radiation fluxes for ecosystems in coastal California. *Theoretical and Applied Climatology*, *144*, 239–252. https://doi.org/10.1007/s00704-021-03518-y

Oliphant, A. J., Dragoni, D., Deng, B., Grimmond, C. S. B., Schmid, H.-P., & Scott, S. L. (2011). The role of sky conditions on gross primary production in a mixed deciduous forest. *Agricultural and Forest Meteorology*, *151*(7), 781–791. https://doi.org/10.1016/j.agrformet.2011.01.005

Oliphant, A. J., & Stoy, P. C. (2018). An Evaluation of Semiempirical Models for Partitioning Photosynthetically Active Radiation Into Diffuse and Direct Beam Components. *Journal of Geophysical Research: Biogeosciences*, *123*(3), 889–901. https://doi.org/10.1002/2017JG004370

Papale, D., Reichstein, M., Aubinet, M., Canfora, E., Bernhofer, C., Kutsch, W., et al. (2006). Toward a standardized processing of Net Ecosystem Exchange measured with eddy covariance technique: Algorithms and uncertainty estimation. *Biogeosciences*, *3*(4), 571–583. https://doi.org/10.5194/bg-3-571-2006

Patrick, L., Cable, J., Potts, D., Ignace, D., Barron-Gafford, G., Griffith, A., et al. (2007). Effects of an increase in summer precipitation on leaf, soil, and ecosystem fluxes of CO_2 and H_2O in a sotol grassland in Big Bend National Park, Texas. *Oecologia*, *151*(4), 704–718. https://doi.org/10.1007/s00442-006-0621-y

Patrignani, A., & Ochsner, T. E. (2015). Canopeo: A powerful new tool for measuring fractional green canopy cover. *Agronomy Journal*, *107*(6), 2312–2320. https://doi.org/10.2134/agronj15.0150

Rastogi, B., Williams, A. P., Fischer, D. T., Iacobellis, S. F., McEachern, K., Carvalho, L., et al. (2016). Spatial and temporal patterns of cloud cover and fog inundation in coastal California: Ecological implications. *Earth Interactions*, *20*(15), 1–19. https://doi.org/10.1175/EI-D-15-0033.1

R Core Team. (2016). *R: A language and environment for statistical computing. R Foundation for Statistical Computing, Vienna, Austria*. URL https://www.R-project.org/

Reinhardt, K., Smith, W. K., & Carter, G. A. (2010). Clouds and cloud immersion alter photosynthetic light quality in a temperate mountain cloud forest. *Botany*, *88*(5), 462–470. https://doi.org/10.1139/B10-008

Ritter, A., Regalado, C. M., & Aschan, G. (2009). Fog reduces transpiration in tree species of the Canarian relict heath-laurel cloud forest (Garajonay National Park, Spain). *Tree Physiology*, *29*(4), 517–528. https://doi.org/10.1093/treephys/tpn043

Rohde, M. M., Froend, R., & Howard, J. (2017). A global synthesis of managing groundwater dependent ecosystems under sustainable groundwater policy. *Ground Water*, *55*(3), 293–301. https://doi.org/10.1111/gwat.12511

Santiago, L. S., & Dawson, T. E. (2014). Light use efficiency of California redwood forest understory plants along a moisture gradient. *Oecologia*, *174*(2), 351–363. https://doi.org/10.1007/s00442-013-2782-9

Schemenauer, R. S., & Cereceda, P. (1994). A Proposed Standard Fog Collector for Use in High-Elevation Regions. *Journal of Applied Meteorology*, *33*(11), 1313–1322. https://doi.org/10.1175/1520-0450(1994)033<1313:apsfcf>2.0.co;2

Staley, D. O., & Jurica, G. M. (1972). Effective atmospheric emissivity under clear skies. *Journal of Applied Meteorology*, *11*, 349–356. https://doi.org/10.1175/1520-0450(1972)011<0349:eaeucs>2.0.co;2

Still, C. J., Riley, W. J., Biraud, S. C., Noone, D. C., Buenning, N. H., Randerson, J. T., et al. (2009). Influence of clouds and diffuse radiation on ecosystem-atmosphere CO_2 and $CO_{18}O$ exchanges. *Journal of Geophysical Research*, *114*, G1. https://doi.org/10.1029/2007JG000675

Torregrosa, A., Combs, C., & Peters, J. (2016). GOES-derived fog and low cloud indices for coastal north and central California ecological analyses. *Earth and Space Science*, *3*(2), 46–67. https://doi.org/10.1002/2015EA000119

Torregrosa, A., O'Brien, T. A., & Faloona, I. C. (2014). Coastal fog, climate change, and the environment. *Eos, Transactions, American Geophysical Union*, *95*(50), 473–474. https://doi.org/10.1002/2014EO500001

Urban, O., Janouš, D., Acosta, M., Czerný, R., Marková, I., Navrátil, M., et al. (2007). Ecophysiological controls over the net ecosystem exchange of mountain spruce stand. Comparison of the response in direct vs. diffuse solar radiation. *Global Change Biology*, *13*(1), 157–168. https://doi.org/10.1111/j.1365-2486.2006.01265.x

Vasey, M. C., Loik, M. E., & Parker, V. T. (2012). Influence of summer marine fog and low cloud stratus on water relations of evergreen woody shrubs (Arctostaphylos: Ericaceae) in the chaparral of central California. *Oecologia*, *170*(2), 325–337. https://doi.org/10.1007/S00442-010.1007/s00442-012-2321-0

Vickers, D., & Mahrt, L. (1997). Quality control and flux sampling problems for tower and aircraft data. *Journal of Atmospheric and Oceanic Technology*, *14*(3), 512–526. https://doi.org/10.1175/1520-0426(1997)014<0512:QCAFSP>2.0.CO;2

Wang, K., & Liang, S. (2009). Global atmospheric downward longwave radiation over land surface under all-sky conditions from 1973 to 2008. *Journal of Geophysical Research*, *114*(D19). https://doi.org/10.1029/2009jd011800

Weathers, K. C., Ponette-González, A. G., & Dawson, T. E. (2020). Medium, vector, and connector: Fog and the maintenance of ecosystems. *Ecosystems*, *23*(1), 217–229. https://doi.org/10.1007/s10021-019-00388-4

Whiteman, C. D., & Allwine, K. J. (1986). Extraterrestrial solar radiation on inclined surfaces. *Environmental Software*, *1*(3), 164–169. https://doi.org/10.1016/0266-9838(86)90020-1

Williams, A. P., Schwartz, R. E., Iacobellis, S., Seager, R., Cook, B. I., Still, C. J., et al. (2015). Urbanization causes increased cloud base height and decreased fog in coastal Southern California. *Geophysical Research Letters*, *42*(5), 1527–1536. https://doi.org/10.1002/2015GL063266

Williams, A. P., Seager, R., Abatzoglou, J. T., Cook, B. I., Smerdon, J. E., & Cook, E. R. (2015). Contribution of anthropogenic warming to California drought during 2012–2014. *Geophysical Research Letters*, *42*, 6819–6828. https://doi.org/10.1002/2015GL064924.Received

Williams, M., Rastetter, E. B., Van der Pol, L., & Shaver, G. R. (2014). Arctic canopy photosynthetic efficiency enhanced under diffuse light, linked to a reduction in the fraction of the canopy in deep shade. *New Phytologist*, *202*(4), 1267–1276. https://doi.org/10.1111/nph.12750

Wu, C., Chen, J. M., Desai, A. R., Hollinger, D. Y., Arain, M. A., Margolis, H. A., et al. (2012). Remote sensing of canopy light use efficiency in temperate and boreal forests of North America using MODIS imagery. *Remote Sensing of Environment*, *118*, 60–72. https://doi.org/10.1016/j.rse.2011.11.012

Xi, X., & Sokolik, I. N. (2012). Impact of asian dust aerosol and surface albedo on photosynthetically active radiation and surface radiative balance in dryland ecosystems. *Advances in Meteorology*, *2012*, 1–15. https://doi.org/10.1155/2012/276207

Xu, L., & Baldocchi, D. D. (2004). Seasonal variation in carbon dioxide exchange over a Mediterranean annual grassland in California. *Agricultural and Forest Meteorology*, *123*(1–2), 79–96. https://doi.org/10.1016/j.agrformet.2003.10.004

Zhang, M., Yu, G.-R., Zhuang, J., Gentry, R., Fu, Y.-L., Sun, X.-M., et al. (2011). Effects of cloudiness change on net ecosystem exchange, light use efficiency, and water use efficiency in typical ecosystems of China. *Agricultural and Forest Meteorology*, *151*(7), 803–816. https://doi.org/10.1016/j.agrformet.2011.01.011